Supplementary material

S.1. *Aramco mech 3.0 model comparison*

Low-temperature chemistry (LTC) can have an effect on the flame structure in the temperature range of 650-800 K, as seen in dimethyl-ether (DME)-air systems (*29*, *30*). Although low-temperature ethylene-air mixtures are expected to be minimally affected by LTC, this assumption was validated by repeating the ethylene-air simulations using an unaltered finite-rate chemistry model that includes LTC reactions.

To assess the effect of LTC on the conditions analyzed here, Cases 2 (Gas-turbine) and 3 (high T) at $\phi = 0.4$ were simulated using the detailed Aramco Mech 3.0 model (*24*) which includes 581 species and 3037 reactions. The Aramco Mech 3.0 model was verified to include the most sensitive reactions in cool-flame propagation as reported by Zhao et al. (*30*).

The temperature and heat release profiles, including the bounds of the total flame thickness and the contribution of main and tail heat release are reproduced for the Aramco Mech 3.0 simulations (see Fig S1). Direct comparisons between the heat release rate and temperature profiles for both Cases 2 and 3 using the two different kinetic models are shown in Figs S2-S3 which reveal near identical temperature profiles but some differences in peak heat release rate.

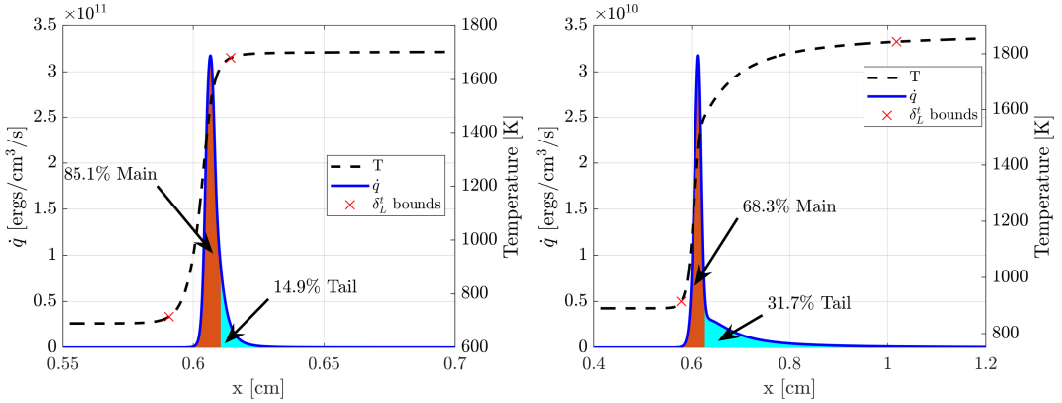

(a) Case 2. (b) Case 3.

Figure S1. Heat release rate and temperature profiles at $\phi = 0.4$ using the Aramco Mech 3.0 model with the total thermal flame thickness and proportions of heat release in the main and tail regions indicated.

.

Relevant flame structure properties are calculated and given below in Table S1. The laminar flame speeds have changed slightly, but the adiabatic flame temperature is nearly identical to the results from USC Mech II. Additionally, while the flame thicknesses have changed, the ratio of the standard flame thickness to the total thermal flame thickness is the same within a few percent. The same applies to the proportion of total heat released in the main region.

Table S1. Some relevant flame properties for Cases 2 and 3 at $\phi = 0.4$ for ethylene-air mixtures simulated with Aramco Mech 3.0.

				Flame length-scales [mm]					
		s_L [cm/s]	T_{ad} [K]	$\delta_{\text{r.l.}}$	δ_f	δ_L^0	δ_L^t	δ_L^0/δ_L^t	$Q_{\text{main}}/Q_{\text{total}}$
Lean	Case 2	14.3	1706	0.045	0.054	0.100	0.237	0.42	0.85
$\phi = \mathbf{0.4}$	Case 3	186.3	1867	0.171	0.105	0.389	4.616	0.08	0.68

Species profiles can be seen in Figs S4-S5. While there are quantitative differences between the USC Mech II and Aramco Mech 3.0 results for some species, the profiles are qualitatively the same exhibiting similar widths and peak locations.

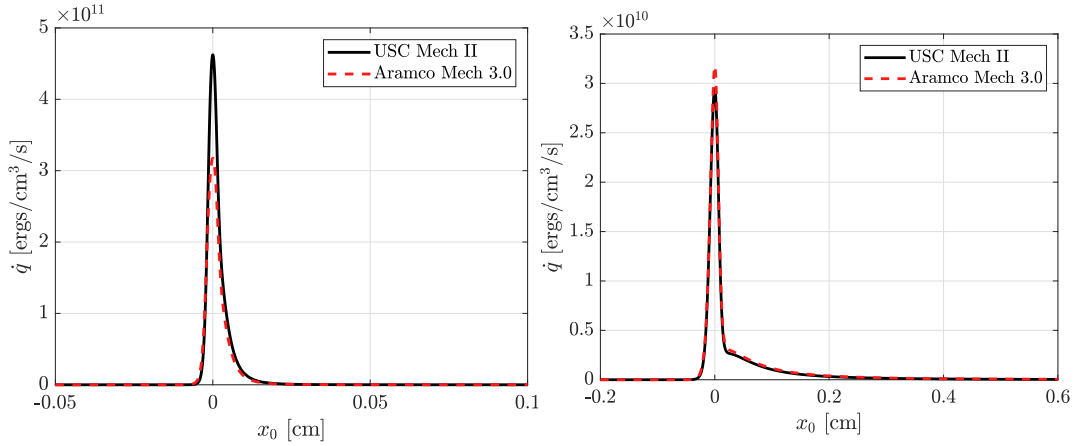

(a) Case 2. (b) Case 3.

Figure S2. Comparison of the heat release profiles for Cases 2 and 3 ($T_u = 690$, 890 K) for $\phi = 0.4$ simulated using the USC Mech II and the Aramco Mech 3.0 models.

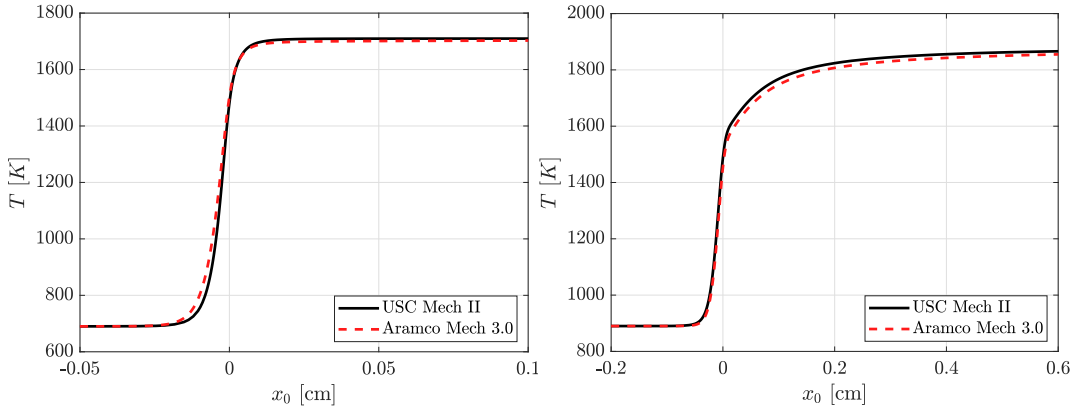

(a) Case 2. (b) Case 3.

Figure S3. Comparison of the temperature profiles for Cases 2 and 3 ($T_u = 690$, 890 K) for $\phi = 0.4$ simulated using the USC Mech II and the Aramco Mech 3.0 models.

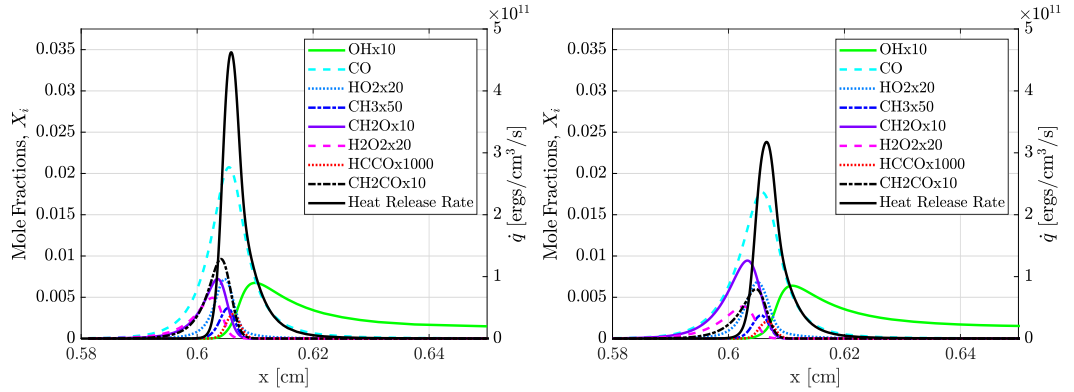

(a) USC Mech II. (b) Aramco Mech 3.0.

Figure S4. Comparison of species profiles for Case 2 ($T_u = 690$ K) at $\phi = 0.4$ simulated using the USC Mech II and the Aramco Mech 3.0 models.

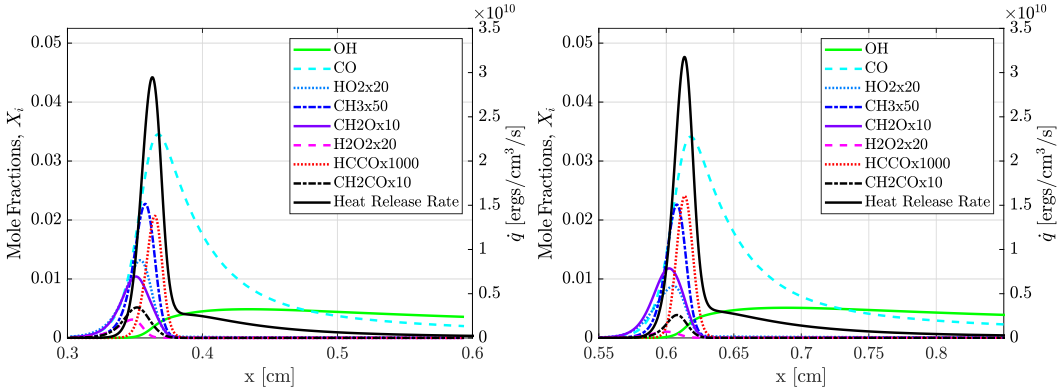

(a) USC Mech II. (b) Aramco Mech 3.0.

Figure S5. Comparison of species profiles for Case 3 ($T_u = 890$ K) at $\phi = 0.4$ simulated using the USC Mech II and the Aramco Mech 3.0 models.

The main heat contributing reactions are also presented here with the same plotting criterion as before: the top three exothermic and top two endothermic reactions in the main and tail regions respectively are identified for Cases 2 and 3 and then plotted across the entire flame structure. This results in a slightly different ranking of key reactions. A summary of the ranked reactions for the two chemical kinetics models for Cases 2 and 3 under lean condition is given in Tables 3-4 and a more detailed discussion is given in Sec. 3.2.1. To enable comparison between the USC MEC II and Aramco Mech 3.0 models the same set of reactions were plotted across the entire flame structure in Figs S6-S7.

While qualitative and quantitative differences in the heat release contributions are thus observed, the key finding of CO+OH $\rightarrow$ CO2+H (R31-USC, R35-Aramco) being the dominant reaction controlling the heat release in the 'long tail' region is reproduced (Fig S7). This is also supported by the high concentrations of CO and OH in the tail region seen in Fig S5.

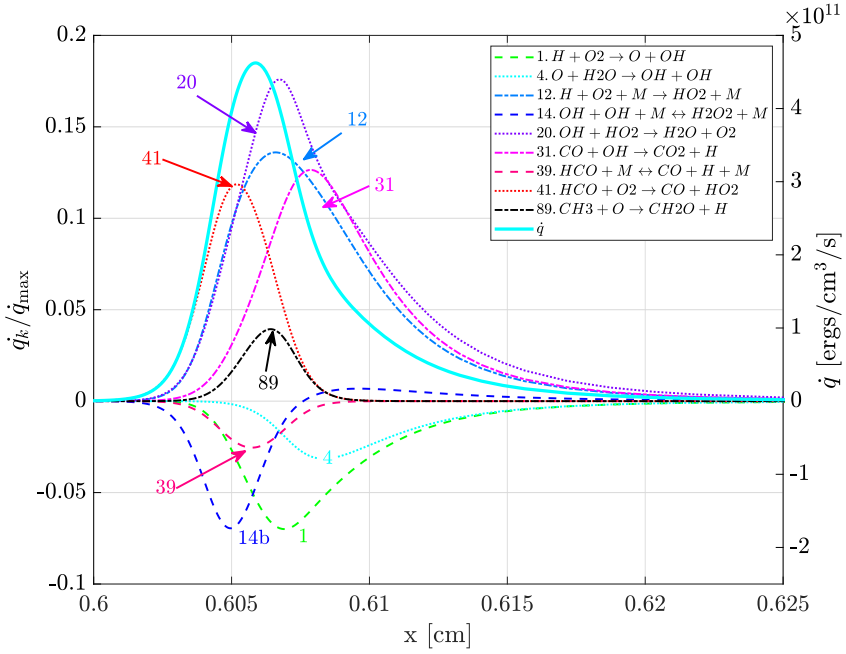

(a) USC Mech II.

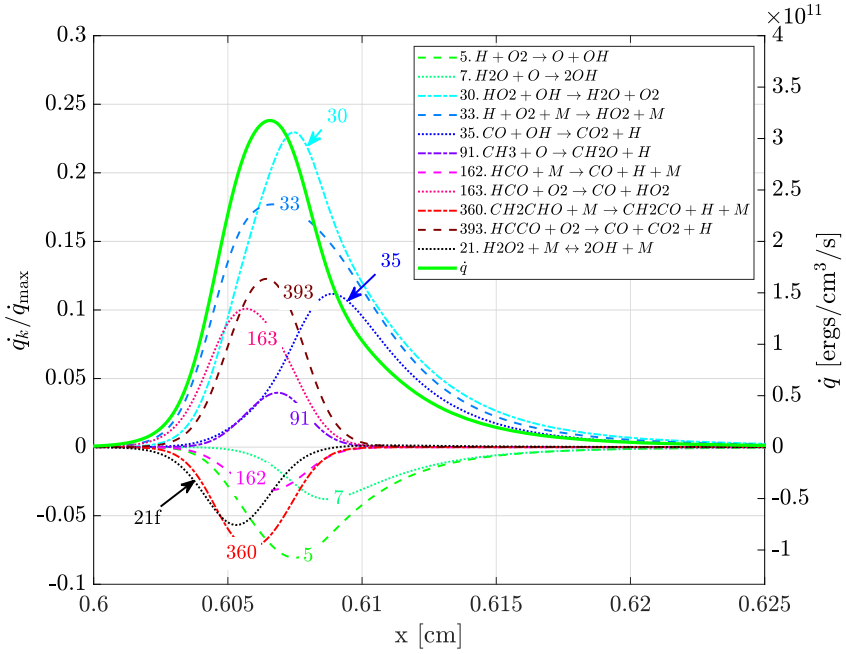

(b) Aramco Mech 3.0.

Figure S6. Heat release rate of individual reactions for Case 2 ($T_u = 690$ K) at $\phi = 0.4$ simulated using the USC Mech II and the Aramco Mech 3.0 model.

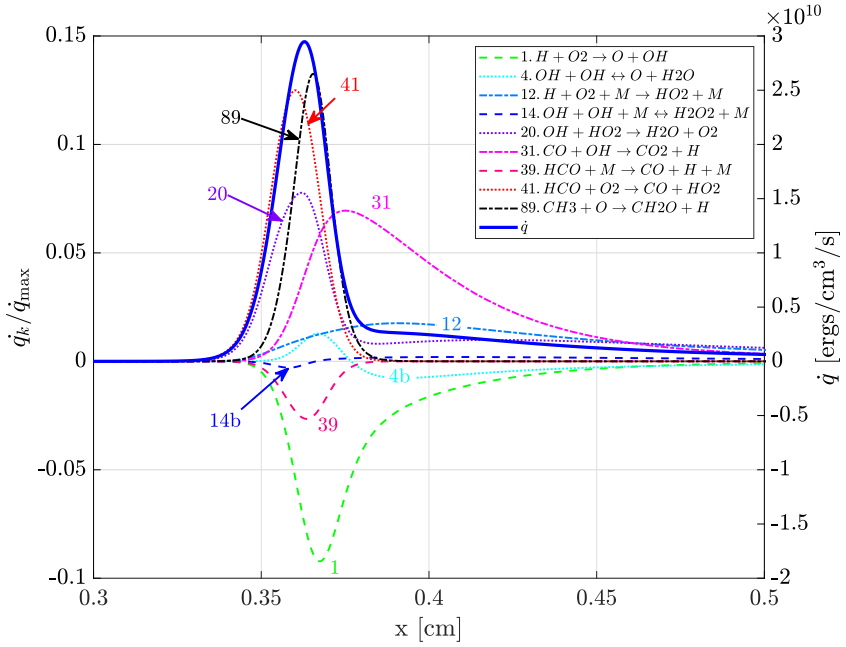

(a) USC Mech II.

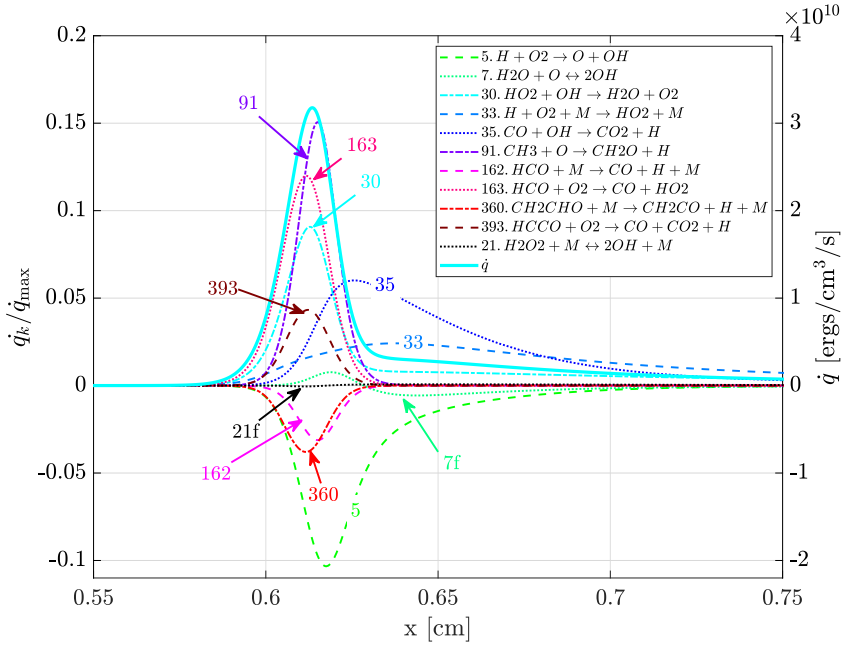

(b) Aramco Mech 3.0.

Figure S7. Heat release rate of individual reactions for Case 3 ($T_u = 890$ K) at $\phi = 0.4$ simulated using the USC Mech II and the Aramco Mech 3.0 model.

S.2. *Laminar, premixed hydrogen-air flame structures*

Analyses of hydrogen-air mixtures were also performed using a H_2 kinetic model proposed by Burke et al. (*23*) (13 species in 27 reactions) and results are presented below. Similar to the ethylene-air flame structure results presented in the main text, hydrogen-air flames show distinct main and tail heat release regions. As expected, Table S2 reveals higher laminar flame speeds and smaller reaction layer and flame structures for hydrogen-air flames. As before,

the diffusion flame thickness is often smaller than the reaction layer thickness indicating it is inappropriate for characterizing the premixed flame structure for calculating non-dimensional parameters. The large discrepancy between total thermal flame thickness and standard flame thickness for Cases 3 and 4 is reproduced.

The temperature and heat release profiles, along with the total thermal flame thickness bounds and proportions of main and tail heat release, for fuel lean, stoichiometric and rich mixtures can be seen in Figs S8-S10. For Cases 2 and 3, the transition to an auto-ignition structure with a convection-reaction balance instead of a convection-diffusion balance preceding a reaction-diffusion balance as in a laminar flame is apparent, and certainly more pronounced than for the ethylene-air mixtures.

Table S2. Some relevant flame properties for all cases considered with H_2 as fuel.

				Flame length-scales [mm]					
		s_L [cm/s]	T_{ad} [K]	$\delta_{\text{r.l.}}$	δ_f	δ_L^0	δ_L^t	δ_L^0/δ_L^t	$Q_{\text{main}}/Q_{\text{total}}$
Lean	Case 1	19.3	1407	0.465	0.338	0.705	1.521	0.46	0.91
	Case 2	52.72	1752	0.017	0.018	0.032	0.072	0.44	0.91
$\phi = \mathbf{0.4}$	Case 3	1030.3	1908	0.398	0.023	0.621	6.184	0.10	0.71
	Case 4	2503.2	2117	0.235	0.008	0.419	7.358	0.06	0.61
Stoich.	Case 1	236.7	2345	0.276	0.035	0.361	7.411	0.05	0.75
	Case 2	741.8	2692	0.010	0.002	0.013	0.106	0.12	0.79
$\phi = \mathbf{1.0}$	Case 3	1650.4	2518	0.297	0.022	0.585	6.031	0.10	0.57
	Case 4	3644.1	2761	0.204	0.008	0.447	8.041	0.06	0.53
Rich	Case 1	308.7	2217	0.268	0.031	0.336	6.302	0.05	0.77
	Case 2	1009.3	2563	0.009	0.002	0.012	0.084	0.14	0.82
$\phi = \mathbf{1.5}$	Case 3	1822.8	2488	0.281	0.024	0.550	5.919	0.09	0.58
	Case 4	3606.8	2736	0.180	0.009	0.392	6.967	0.06	0.53

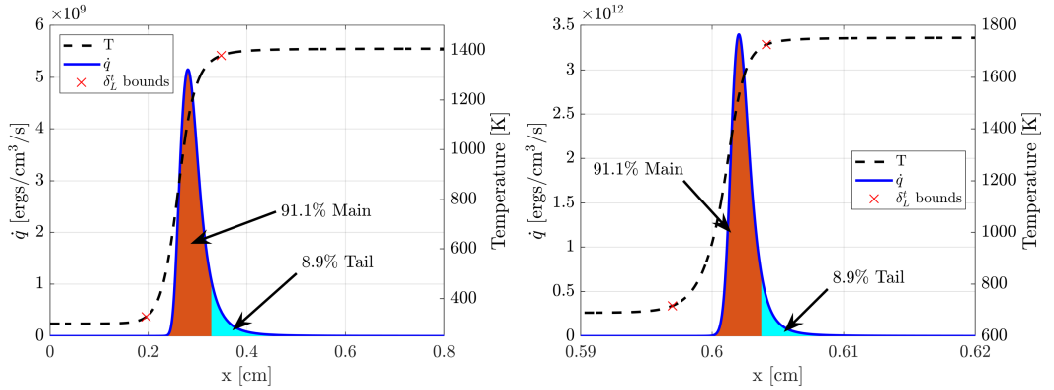

(a) Case 1.

(b) Case 2.

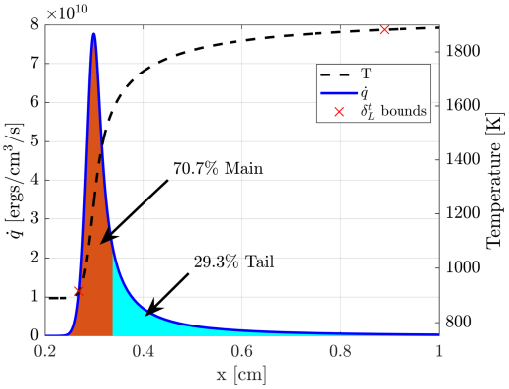

(c) Case 3.

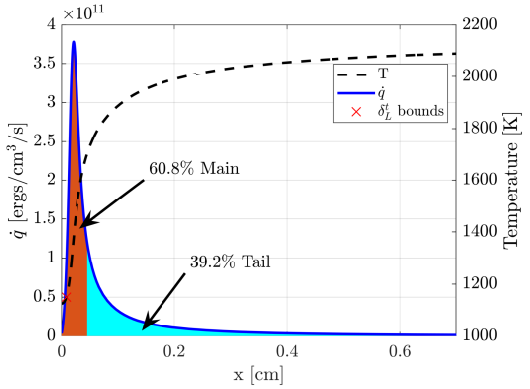

(d) Case 4.

Figure S8. Heat release rate and temperature profiles at $\phi = 0.4$ for a hydrogen-air mixture with the total thermal flame thickness and the proportions of heat release in the main and tail regions indicated.

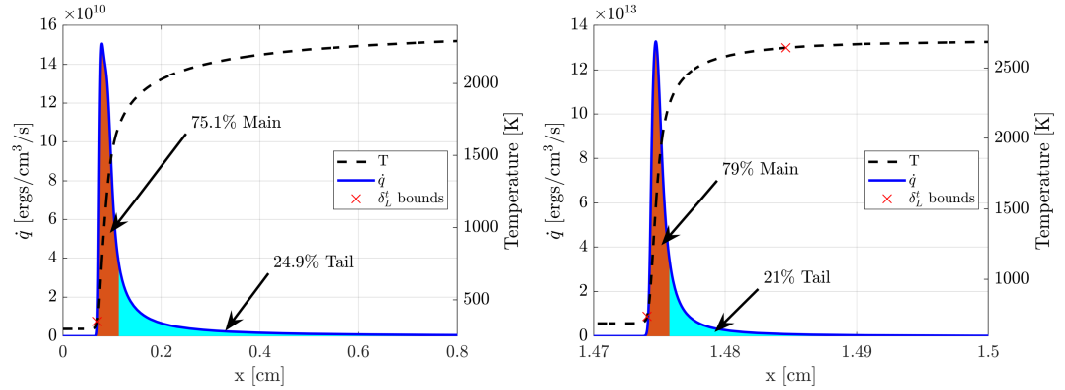

(a) Case 1.

(b) Case 2.

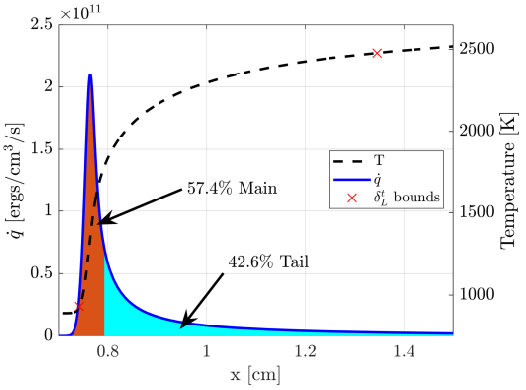

(c) Case 3.

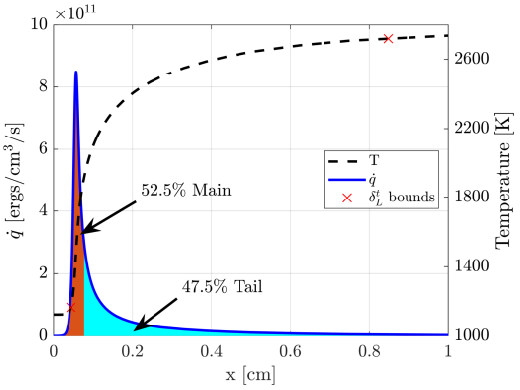

(d) Case 4.

Figure S9. Heat release rate and temperature profiles at $\phi = 1.0$ for a hydrogen-air mixture with the total thermal flame thickness and the proportions of heat release in the main and tail regions indicated.

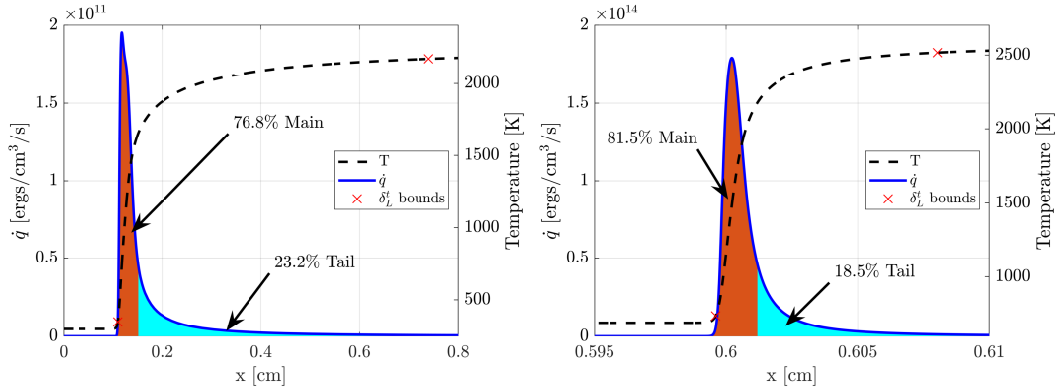

(a) Case 1.

(b) Case 2.

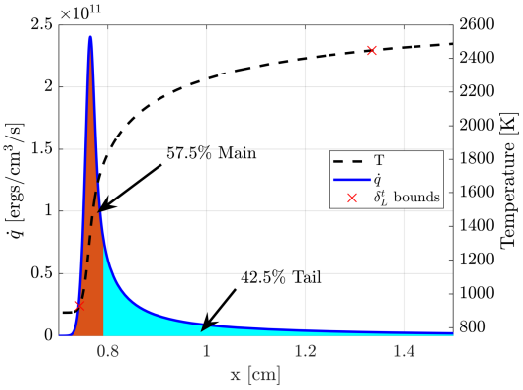

(c) Case 3.

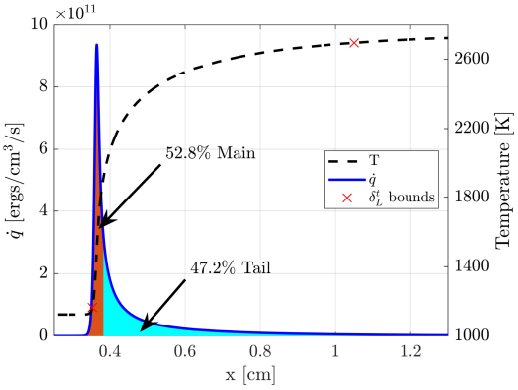

(d) Case 4.

Figure S10. Heat release rate and temperature profiles at $\phi = 1.5$ for a hydrogen-air mixture with the total thermal flame thickness and the proportions of heat release in the main and tail regions indicated.